Tribology International 117 (2018) 112–118

Contents lists available at ScienceDirect

Tribology International

journal homepage: www.elsevier.com/locate/triboint

Multi-pass micro-scratching and tribological behaviors of an austenitic steel in media

Qilong Wei *, Jiangang Lü, Qiang Yang, Xiaoyuan Li

Institute of Machinery Manufacturing Technology, CAEP, Mianyang, China

ARTICLE INFO

Keywords:
Micro-scratch
Nano-ceria slurry
Coefficient of friction
Depth increment

ABSTRACT

Micro-scratching and tribological behaviors of an austenitic steel in media including a nano-caria slurry, a carrier liquid and air are researched thoroughly, with the purpose to provide a technical method for simulation of microscopic mechanisms in polishing. It is found that penetration depth increment and remnant depth increment are highest in the first pass and they decrease markedly in later passes, while coefficient of friction decreases with pass. Both penetration depth increment and coefficient of friction are maximal in the nano-ceria slurry. Based on the Hertzian theory, it can be deduced that multi-pass scratch transforms interaction form between indenter and surface, while the particles are embedded into the softer surface under higher load, both of which influence latter scratch.

1. Introduction

Polishing is a key technology which endows material surfaces with optical properties and other functions, and it has played important roles in various scientific and technological fields [1–3]. Development of new technologies has brought forward more and more high requirements on polishing of surfaces. For example, extreme ultraviolet photo-mask blank requires surface roughness less than 0.15 nm [4,5], and super-polish aspheres require surface roughness less than 0.2 nm [6]. These rigorous requirements demand both advanced polishing methods and scientific understanding of polishing.

In polishing process there are complex three-body interactions among abrasive particles, polishing pad and material surfaces, where a large number of abrasive particles are constrained weakly by polishing pads. In some extreme conditions, polishing pad constrains abrasive particles so strongly that the situation is simplified to a two-body interaction. According to constraints from polishing pad, abrasive particles remove material by plowing or rolling [7–9]. Thus concourse of large number of abrasive particles removes material macroscopically and creates smooth surface.

The basic material removal has been researched by simulation with AFM and scratch methods, where a sphere glued to the tip scratches material surfaces, or the tip scratches material surfaces directly. Komanduri et al. scratched on single-crystal aluminum with a tip with radius 25 nm in AFM, and found that material was removed by a plowing method when scratch depth was very small [10]. Beake et al. conducted nano-scratch on a single-crystal silicon with a spherical indenter of 4.6 μm in radius, and obtained the critical fracture load and toughness-brittleness transformation characters [11]. Zhang et al. onducted nano-scratch on a KDP crystal, and found that it was the non-uniform deformation of material before the indenter that produced marked fluctuations of friction force and coefficient of friction [12]. But these researches all reduce the three-body conditions in polishing process to two-body conditions, which are different from actual polishing conditions and produce results with large deviations.

Many researchers analyzed polishing process with micro-scratch method, but they did not take abrasive particles into consideration. For example, Demirci et al. simulated polishing of glasses by triple scratch test, and found that distance between scratches and scratching speed had marked influences on formation of chips and material removal [13]. Gu et al. also studied influence of separation distance between parallel scratches on material removal of BK7 glass [14]. There lacks of research on scratch in suspensions of small particles and multi-pass scratch, which both are key characters in polishing processes.

In fact, micro-scratch technology is more suitable to simulate the three-body conditions in polishing process, as it has more suited radius ratio of the indenter and abrasive particles. Size of abrasive particles usually is about 100 nm, while radius of spherical indenter is about 5 μm for nano-scratch and 10–100 μm for micro scratch [15,16], which means that indenter size of micro scratch is about 100–1000 times of size of

* Corresponding author.
E-mail address: weiqilong2004@126.com (Q. Wei).

http://dx.doi.org/10.1016/j.triboint.2017.08.016
Received 7 January 2017; Received in revised form 24 April 2017; Accepted 16 August 2017
Available online 18 August 2017

abrasive particles. Then it can ensure that there are enough particles participating in the three-body interactions under the indenter when micro-scratch is conducted in abrasive slurries.

Some researchers studied the microscopic three-body conditions by simulation with nano-scratch in slurries. For example, Fu et al. [17] glued a silica sphere with radius 400 nm on the AFM tip, and scratched copper films with it in various media including air, de-ionized water, and silica slurry with mean particle size 110 nm. He obtained variations laws of depth, friction force and wear rate with media, and determined contributions from slurry chemistry and liquid buoyancy. But he did not consider radius ratio of glued silica sphere and sphere in slurry, as there could not have enough abrasive particles which participated in friction between glued sphere and copper films.

On the other hand, multi-pass scratch which is done on the same location repeatedly can simulate repeated movements of abrasive particles in polishing by and large. But micro-scratch do not have high signal-to-noise as nano-scratch, which may make it difficult to distinguish and exhibit results with small differences in scratching on hard and brittle materials such as K9 and fused silica. As single-phase austenitic steels have low hardness and high plasticity, they are good candidates for scratching, which will provide better scientific and technological bases for researching on hard and brittle materials.

Besides, as physical meanings are not clear for penetration depth and remnant depth during multi-pass scratch, a group of six parallel scratches and a perpendicular scanning will be conducted.

2. Experiments and materials

An austenitic steel (AS) specimen and a slurry of ceria particles were used in micro-scratch experiments. Fig. 1(a) shows a microscopic image the AS, and it is found that grains are near equi-axial with size between 10 μm and 100 μm. Fig. 1(b) shows a TEM image of ceria particles, and it indicates that the particles are irregular polyhedrons with size between 100 nm and 200 nm.

An aqueous solution of sodium carboxymethyl cellulose and sodium nitrite was used as the carrier liquid (CL). A ceria slurry with particles weight concentration 1% was prepared by dispersing the nano-ceria particles into the CL with an ultrasonic probe. Thus media used in experiments included the nano-ceria slurry, the carrier liquid, and air.

A micro scratch tester of CMS Instruments was adopted in micro-scratch experiments, and the diamond indenter was a spherical Rockwell one with a tip of 100 μm in radius. An advanced scratch mode was selected, with both pre-scan load and post-scan load 0.03 N, scratch length 2.0 mm, scratch speed 2.0 mm/min, acquisition rate 30 Hz.

Before scratching, microscopic characters on the sample surface were observed by optical microscopy of the tester, and locations without obvious defects, polishing tracks and contamination were chosen to be used in experiments.

Firstly, six-pass scratching with constant loads from 0.5 N to 2.0 N was done in air. Then another group of scratch experiments were conducted in air by the manner shown in Fig. 2, to obtain dimensions of impressions. Six parallel strips were scratched with load 2.0 N and pass from 1 to 6, distance between nearby strips about 300 μm. Then four parallel strips perpendicular to these six strips were scratched with distance 200 μm–300 μm (P-scan A), and additional two parallel strips were scratched in the same direction outside the six parallel strips with distance 200 μm–300 μm (P-scan B).

Six-pass scratch with constant load 2.0 N was done in the CL and the nano-ceria slurry respectively. The slurry or CL was added onto selected locations before scratch, and was cleaned with filter paper after scratch. Besides, the indenter was cleaned with de-ionized water in an ultrasonic bath after each group of scratches and dried with filter paper.

3. Experimental results

Fig. 3(a) shows results of the first scratch on the austenitic steel with a constant load 1.0 N in air, where P_d, R_d and μ are penetration depth, remnant depth after elastic recovery, and coefficient of friction respectively. It is found that P_d, R_d and μ all fluctuate in different ranges, and P_d and R_d fluctuate synchronously. Average values of P_d, R_d and μ in the total length of 2.0 mm are 1.401 μm, 0.930 μm and 0.15 respectively, while their relative standard deviation (rsd) are 5.99%, 10.1% and 8.31% respectively. In the latter sections, P_d, R_d and μ are used to represent their average values.

Fig. 3(b) shows statistical results of all first scratches on the austenitic steel with different constant loads in air. It is found that when the load increases from 0.5 N to 2.0 N, P_d, R_d and μ all increase monotonously, with the maximal increased percentage 244%, 227%, and 52.3%

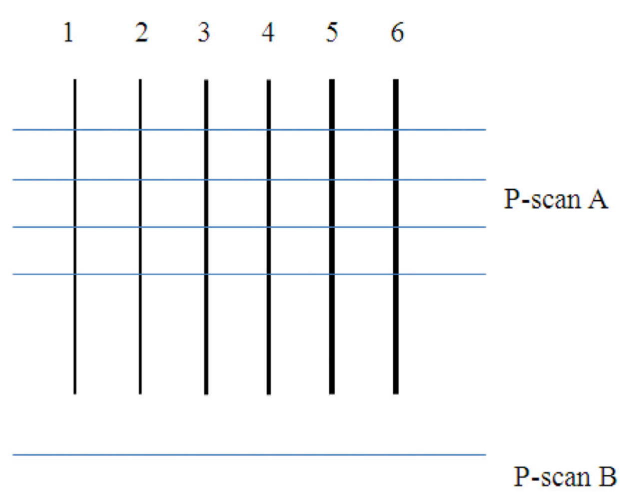

Fig. 2. Schematic of the six parallel strips and perpendicular scanning.

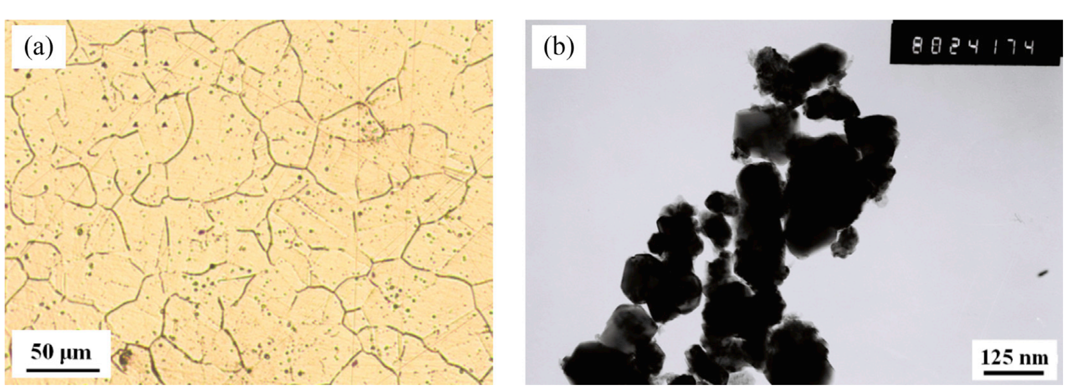

Fig. 1. Microscopic images of (a) the austenitic steel and (b) the ceria particles.